The Journal of Immunology

In Utero Exposure to Histological Chorioamnionitis Primes the Exometabolomic Profiles of Preterm CD4$^+$ T Lymphocytes

Poojitha Matta, Stacy D. Sherrod, Christina C. Marasco, Daniel J. Moore, John A. McLean and Joern-Hendrik Weitkamp

J Immunol 2017; 199:3074-3085; Prepublished online 25 September 2017;
doi: 10.4049/jimmunol.1601880
http://www.jimmunol.org/content/199/9/3074

The Journal of Immunology is published twice each month by
The American Association of Immunologists, Inc.,
1451 Rockville Pike, Suite 650, Rockville, MD 20852

Print ISSN: 0022-1767 Online ISSN: 1550-6606.

In Utero Exposure to Histological Chorioamnionitis Primes the Exometabolomic Profiles of Preterm CD4$^+$ T Lymphocytes

Poojitha Matta,* Stacy D. Sherrod,† Christina C. Marasco,‡ Daniel J. Moore,* John A. McLean,† and Joern-Hendrik Weitkamp*

Histological chorioamnionitis (HCA) is an intrauterine inflammatory condition that increases the risk for preterm birth, death, and disability because of persistent systemic and localized inflammation. The immunological mechanisms sustaining this response in the preterm newborn remain unclear. We sought to determine the consequences of HCA exposure on the fetal CD4$^+$ T lymphocyte exometabolome. We cultured naive CD4$^+$ T lymphocytes from HCA-positive and -negative preterm infants matched for gestational age, sex, race, prenatal steroid exposure, and delivery mode. We collected conditioned media samples before and after a 6-h in vitro activation of naive CD4$^+$ T lymphocytes with soluble staphylococcal enterotoxin B and anti-CD28. We analyzed samples by ultraperformance liquid chromatography ion mobility–mass spectrometry. We determined the impact of HCA on the CD4$^+$ T lymphocyte exometabolome and identified potential biomarker metabolites by multivariate statistical analyses. We discovered that: 1) CD4$^+$ T lymphocytes exposed to HCA exhibit divergent exometabolomic profiles in both naive and activated states; 2) ∼30% of detected metabolites differentially expressed in response to activation were unique to HCA-positive CD4$^+$ T lymphocytes; 3) metabolic pathways associated with glutathione detoxification and tryptophan degradation were altered in HCA-positive CD4$^+$ T lymphocytes; and 4) flow cytometry and cytokine analyses suggested a bias toward a T_H1-biased immune response in HCA-positive samples. HCA exposure primes the neonatal adaptive immune processes by inducing changes to the exometabolomic profile of fetal CD4$^+$ T lymphocytes. These exometabolomic changes may link HCA exposure to T_H1 polarization of the neonatal adaptive immune response. ***The Journal of Immunology*****, 2017, 199: 3074–3085.**

Preterm birth remains the leading cause of neonatal morbidity and mortality in the United States (1) and across the globe (2). The most common causes include spontaneous preterm labor and premature rupture of membranes (3). Both share a close association with histological chorioamnionitis (HCA) (4–6), an inflammation of the fetal membranes typically caused by intrauterine bacterial infection (7). Fetal exposure to HCA induces in utero immune activation, resulting in fetal inflammatory response syndrome (FIRS), and shapes the neonatal transcriptomic immune response (8–10). Clinical characteristics of FIRS consist of systemic inflammation and elevation of fetal plasma IL-6 and other proinflammatory cytokine levels (11). Long-term sequelae of the sustained systemic inflammation precipitated by fetal exposure to HCA include blindness (12), cerebral palsy (13), impaired cardiac function (14), lung disease (15), and disruption of normal fetal immune development (16–20).

Recent studies on fetal sheep have demonstrated activation of the adaptive immune system after exposure to HCA (21). Furthermore, umbilical cord blood derived from human neonates with clinical evidence of perinatal infection exhibited a higher proportion of T_H1 cells than umbilical cord blood from uninfected neonates (22). Activation and differentiation of CD4$^+$ T lymphocytes is thought to be tightly regulated by cellular metabolism (23). However, data on metabolic changes induced by premature activation of fetal CD4$^+$ T lymphocytes remain limited. This deficit hinders the identification of therapeutic targets and further research on the severe and lifelong complications of premature birth after exposure to HCA.

Within the adaptive immune system, naive and activated CD4$^+$ T lymphocytes communicate through many different means, mediating their effects and thereby ensuring the production of an effective immune response. The secretion of metabolites constitutes one such critical mode of intercellular communication because molecular secretions often provide direction for and regulate collective cellular actions including naive CD4$^+$ T lymphocyte activation and proliferation. Thus, the ability to study molecular secretions in the developing fetal adaptive immune system may provide insight into normal and atypical aspects of fetal adaptive immune processes resulting from fetal exposure to HCA.

*Department of Pediatrics, Vanderbilt University Medical Center, Monroe Carell Jr. Children's Hospital at Vanderbilt, Nashville, TN 37232; †Department of Chemistry, Vanderbilt University, Nashville, TN 37235; and ‡Department of Physics, Vanderbilt University, Nashville, TN 37235

ORCIDs: 0000-0003-0324-9314 (C.C.M.); 0000-0002-6889-9345 (D.J.M.).

Received for publication November 7, 2016. Accepted for publication August 23, 2017.

This work was supported by the Eunice Kennedy Shriver National Institute of Child Health and Human Development (Grant HD061607 to J.-H.W.), the National Institutes of Health National Center for Advancing Translational Sciences (Grant 5UH3TR000491-04 to S.D.S.), and the Department of Pediatrics, Vanderbilt University Medical Center. The REDCap database was utilized for data collection and analysis through Clinical and Translational Science Award UL1 TR000445 from the National Institutes of Health National Center for Advancing Translational Sciences. The contents of this manuscript are solely the responsibility of its authors and do not necessarily represent the official views of funding agencies and/or organizations. In addition, the relevant funding agencies and organizations had no role in the experimental design, collection, analysis, or interpretation of data, nor were they involved in the writing of the manuscript and the decision to submit for publication.

Address correspondence and reprint requests to Dr. Joern-Hendrik Weitkamp, Monroe Carell Jr. Children's Hospital at Vanderbilt, 2200 Children's Way, 11114 Doctor's Office Tower, Nashville, TN 37232-9544. E-mail address: hendrik.weitkamp@vanderbilt.edu

The online version of this article contains supplemental material.

Abbreviations used in this article: DA, dopamine; DOL, day of life; FA, formic acid; FC, fold change; FIRS, fetal inflammatory response syndrome; GSH, glutathione; HCA, histological chorioamnionitis; 3-HK, 3-hydroxykynurenine; 4-HNE, 4-hydroxynonenal; 5-HT, serotonin; IM-MS, ion mobility–mass spectrometry; LC-MS, liquid chromatography–MS; LPC, LysoPC [18:2(9Z, 12Z)]; m/z, mass-to-charge; NE, norepinephrine; OPLS-DA, orthogonal partial least squares–discriminant analysis; PLA_2, phospholipase A_2; RT, retention time; SEB, staphylococcal enterotoxin B; UPLC, ultraperformance LC.

We sought to assess changes in the exometabolomic profiles of fetal naive $CD4^+$ T lymphocytes exposed to HCA after in vitro activation, using ion mobility–mass spectrometry (IM-MS), a highly specific analytical process that allows for small-volume, complex biological samples to be analyzed with a high-throughput and unbiased approach. After comparing the exometabolomic profiles of fetal $CD4^+$ T lymphocytes isolated from matched HCA-positive and -negative infants, we putatively identified metabolites and candidate biochemical pathways that may function as biomarkers of HCA-induced reconditioning of fetal adaptive immune processes. These metabolic pathways may also function as possible targets for the prevention of inflammatory sequelae resulting from in utero exposure to HCA.

Materials and Methods

Experimental design

Sample collection and study populations. This study was approved by the Vanderbilt University Medical Center Institutional Review Board (protocols 090161 and 110833). PBMCs were collected prospectively from premature infants admitted to Vanderbilt University Medical Center neonatal intensive care unit on postnatal days 3, 7, 14, and 28. PBMCs were isolated and stored in liquid nitrogen. From this repository, we identified 10 individual samples of preterm patients exposed to HCA and 10 individual HCA-negative samples with similar gestational age, race, sex, and mode of delivery (Table I). All 20 mothers received prenatal steroids; most were exposed to prenatal antibiotics. All patients were exposed to postnatal antibiotics. Presence of funisitis in HCA-positive patients was determined upon review of the surgical pathology report. Two sample *t* tests assuming unequal variances were conducted on each variable to determine statistical similarity/difference between the two sample groups.

Naive $CD4^+$ T lymphocyte purification and activation. We isolated naive $CD4^+$ T lymphocytes from PBMCs using an indirect magnetic labeling system (Miltenyi Biotec, Auburn, CA), as previously reported (24). In brief, $CD45RO^+$ and non-$CD4^+$ T lymphocytes were magnetically labeled using a biotin-conjugated Ab and anti-biotin microbead mixture, according to manufacturer's instructions. Isolation of naive $CD4^+$ T lymphocytes is achieved by depletion of magnetically labeled cells with ≥90% purity.

After sorting, the cell suspension was centrifuged to remove sorting buffer and resuspended in RPMI 1640 medium supplemented with 10% Human AB Serum (Sigma, St. Louis, MO) and 1% penicillin-streptomycin (Thermo Fisher, Grand Island, NY). We cultured purified naive $CD4^+$ T lymphocytes in 96-well microtiter plates, 40,000 cells per well. Immediately after plating, we collected 100 μl of conditioned media from all samples. Naive $CD4^+$ T lymphocytes were subsequently activated using 30 μl of soluble staphylococcal enterotoxin B (SEB; 1 μg/ml, kindly provided by Dr. M.J. Rosen, Cincinnati Children's Hospital Medical Center) and 30 μl of anti-CD28 (10 μg/ml; BD Biosciences, San Jose, CA) (25). After 6 h of incubation, at 37°C, 100 μl of reconditioned media was collected from all samples and stored at −80°C (Supplemental Fig. 1A) (26).

Sample preparation for mass spectrometry. Samples were prepared for reverse-phase (C_{18}) IM-MS and analyzed as previously reported (27); they are shown in Supplemental Fig. 1B. In brief, we performed a cold methanol (Optima liquid chromatography–MS [LC-MS] grade; Fisher Scientific, Pittsburgh, PA) protein precipitation and dried the supernatants in vacuo (SpeedVac concentrator; Thermo Fisher). Desiccates were reconstituted in 100 μl of 0.1% formic acid (FA) in water (LC-MS grade; Fisher Scientific). Quality-control samples were prepared by combining equal volumes (15 μl) of each sample.

Mass spectrometry. Ultraperformance LC (UPLC)-IM-MS and data-independent acquisition were performed on a Waters Synapt G2 (Waters, Milford, MA) mass spectrometer equipped with a Waters nanoAcquity UPLC system and autosampler (Waters). Metabolites were separated on a 1 mm × 100 mm T3 column packed with 1.8-μm, 10-nm high-strength silica particles (Waters). Liquid chromatography was performed using a 25-min gradient at a flow rate of 70 μl/min using solvent A (0.1% FA in H_2O) and solvent B (0.1% FA with acetonitrile). Ninety-nine percent of solvent A is initially perfused with a linear gradient applied such that solvent A is decreased to 1% and solvent B increased to 99% over 12 min. This condition is held for 3 min. The solvent percentage is then returned to the initial state in the next minute (99% solvent A, 1% solvent B) and held for 9 min to re-equilibrate the column.

Typical IM-MS analyses were run using resolution mode, with a capillary voltage of 3 kV, source temperature at 120°C, sample cone at 35, desolvation temperature at 400°C, He cell flow of 180 ml/min, and an IM gas flow of 90 ml/min. The data were acquired in positive ion mode from 50 to 2000 Da with a 0.5-s scan time; full-scan data were mass corrected during acquisition using an external reference consisting of 3 ng/ml solution of leucine enkephalin. All analytes were analyzed using an instrument acquisition mode called elevated-energy MS with an energy ramp from 5 to 35 eV.

Analysis strategy

Data processing. We converted acquired raw data to mzXML format using the Proteowizard msconvert tool (http://proteowizard.sourceforge.net/team.shtml) (28). These files were then analyzed using the "XCMS" platform in the R Studio statistical package, to peak pick and align features (i.e., retention time [RT] and mass-to-charge [m/z] ratio pairs). XCMS was used with default settings (as described on The Scripps Research Institute Web site: https://metlin.scripps.edu/landing_page.php?pgcontent=mainPage) except rector (method = "obiwarp"). Data were normalized to the summed total ion intensity per chromatogram, with the total ion count normalized to 10,000 counts.

Determination of exometabolomic differences. We analyzed the processed data matrix with multivariate statistical analysis using Umetrics extended statistics software EZInfo version 2.0.0.0 (Waters). Orthogonal partial least squares–discriminant analysis (OPLS-DA) was performed on expression levels of all measurable analytes and used Pareto scaling to determine exometabolomic differences between HCA-positive and -negative samples in the naive and activated states.

The integrated intensity of each chromatographically resolved m/z peak was $\log_2$ transformed. Change in peak area after $CD4^+$ T lymphocyte activation was determined using fold change (FC) (where $FC = mean_{ACTIVATED}/mean_{NAIVE}$). Statistical significance was determined using a paired two-tailed Student *t* test. Technical replicates were used in these calculations; all calculations were performed on $\log_2$ transformed values. An m/z species was considered differentially expressed when it met the dual criteria of $|FC| > 1$ and $p < 0.05$ (for all subsequent analyses, $p < 0.05$ was used as the threshold for significance). Direction of change was defined as $FC > 1$ = produced and $FC < -1$ = consumed. In addition, for a differentially expressed metabolite to be changed because of HCA exposure, it had to exhibit a magnitude difference ($|FC| > 1$) and $p < 0.05$ from control samples.

Identification of analytes by IM-MS. Volcano plot analyses were generated to compare exometabolomic differences between HCA-positive and -negative samples and to determine metabolites of interest. The $\log_2[FC]$ between HCA-positive and -negative samples was plotted along the *x*-axis and calculated using normalized abundance values. The *p* values were calculated using an unpaired two-tailed Student *t* test of equal variance to determine statistical significance of difference of group means values. Metabolites that showed a *p* value <0.05 were prioritized for identification. All analyses were performed on $\log_2$ transformed values.

Putative metabolite identifications were assigned using both monoisotopic accurate mass measurements (<30 ppm) and fragmentation data (tandem MS analyses). Candidate structures were obtained and interpreted with available databases, including the Human Metabolome Database (29), METLIN (30), and LIPID MAPS (31). In addition, acquired raw data were analyzed using Progenesis QI (32), a small-molecule discovery analysis software for LC-MS data.

The statistical significance of putatively identified metabolites was analyzed between matched disease and control pairs. Significance was determined using two-way repeated-measures (mixed-model) ANOVA. Wilcoxon matched-pairs signed-rank tests were performed to determine the overall statistical significance between pairwise comparisons. All calculations were performed on ($\log_2$ transformed) normalized abundance values in GraphPad Prism.

Analysis of $CD4^+$ T lymphocyte cytokine production and phenotype

Flow cytometry. We analyzed phenotype, activation, and cytokine profiles of $CD4^+$ T lymphocytes using multicolor flow cytometry. We stained viable cryopreserved PBMCs collected at postnatal days 3, 7, 14, and 28 using the following Ab panel: CD3, CD4, CD8, CD45RO, CD25, CD69, LFA-1, CD154 (CD40 ligand), CD127, FOXP3, GARP, CCR4, CCR6, and CXCR3. An amine-reactive live-dead marker was used to exclude dead cells. A Becton Dickson LSR-II flow cytometer and FlowJo software (Tree Star) were used to analyze the data. Subsets of $CD4^+$ T lymphocytes were characterized using the following markers (33): T_H1 ($CD45RO^+$ $CXCR3^+$ $CCR6^-$ $CCR4^-$). A comparable staining panel was used in a recent study to identify activated memory T_H1 and T_H2 lymphocytes in the cord blood of healthy term neonates (34).

Activation assay and analysis of cytokine production. Using the same repository as described earlier, we identified five individual preterm infants exposed to HCA and five individual HCA-negative patients matched for

gestational age, race, sex, mode of delivery, day of blood draw, and prenatal steroid exposure.

We isolated naive $CD4^+$ T lymphocytes from PBMCs using an indirect magnetic labeling system (Miltenyi Biotec), as detailed earlier. We cultured purified naive $CD4^+$ T lymphocytes in 96-well microtiter plates, 40,000 cells per well. Immediately after plating, we collected 100 μl of conditioned media from all samples. Naive $CD4^+$ T lymphocytes were subsequently activated using 10 ng/ml PMA (Sigma) and 1 μg/ml ionomycin (Sigma). After 6 h of incubation, at 37°C, 100 μl of reconditioned media was collected from all samples. We confirmed >95% cell viability at the end of the incubation period in our pilot experiments. Cytokines were subsequently measured using the Milliplex Map multiplex magnetic bead-based immunoassay kits (Millipore) on a Luminex Flexmap 3D Platform as reported previously (35). A paired *t* test was used to determine the statistical significance of differences in IFN-γ secretion.

Results

$CD4^+$ T lymphocytes of preterm infants exposed to HCA exhibited distinct exometabolomic signatures in both naive and activated states

The mean gestational age at birth was nearly identical between both groups: HCA-positive: 27 wk; HCA-negative: 26 wk, 6 d ($p = 0.69$). The male-to-female ratio was identical in both groups ($p = 1$). The HCA-positive group had four African-American samples and the HCA-negative group had two; the remaining samples were white ($p = 0.36$). The HCA-positive group had equal proportions of cesarean and vaginal deliveries, whereas the HCA-negative group had two vaginal deliveries and eight cesareans ($p = 0.18$). The day of blood draw showed a statistically significant difference between the two groups ($p = 0.04$), whereas the differences in exposure to prenatal antibiotics were statistically insignificant ($p = 0.15$). All patients were exposed to postnatal antibiotics, particularly ampicillin and gentamicin, at least through day of life (DOL) 2. Notably, HCA-positive patients were exposed to antibiotics for a statistically longer period than HCA-negative patients ($p = 0.03$) (Table I). All 20 mothers received prenatal steroids to promote fetal lung development. Histological signs of funisitis were found in 8 of 10 HCA-positive patients. Seven patients showed signs of stage II FIRS, and one patient showed signs of stage I FIRS.

After data processing (peak picking and alignment), we detected 1652 unique exometabolomic features (each feature presents a unique combination of m/z ratio and RT). To study the metabolomic signatures of each sample type and differences between HCA-positive and -negative sample groups, we carried out a series of statistical analyses on all detected exometabolomic features.

We used OPLS-DA to examine what, if any, differences exist between the exometabolomic signatures of HCA-positive and -negative samples. The OPLS-DA score plots in Fig. 1 display the exometabolomic signatures of each sample type. Fig. 1A shows the exometabolomic signature of naive $CD4^+$ T lymphocytes, that is, before SEB/CD28-induced activation, and Fig. 1B depicts the exometabolomic signature of activated $CD4^+$ T lymphocytes. Fig. 1A demonstrates a distinct separation between HCA-positive and -negative sample groups along OPLS1, resolving the two sample types into two discrete classes. This unambiguous between-group difference suggests sizable variations in the exometabolomic signatures of HCA-positive and -negative samples in the naive state. Interestingly, the HCA-negative samples exhibit separation along OPLS2, suggesting a unique within-group variation not seen in the HCA-positive sample group. The two sample groups were similarly discretized along OPLS1 in the activated state (Fig. 1B), suggesting continued disparities in the exometabolomic signatures of HCA-positive and -negative sample groups. The sizable within-group variation unique to the HCA-negative sample group persisted in the activated state.

We compared HCA-negative samples collected 5 d postnatal ($n = 4$) with samples collected 10 d postnatal ($n = 6$) for any potential bias. We determined that these HCA-negative samples behaved similarly, regardless of the date of sample collection. Therefore, the within-group variation exhibited by the HCA-negative sample group cannot be explained by the timing of sample collection.

The global exometabolomic profiles of both sample types were significantly altered in response to SEB/CD28 stimulation. To directly compare the production and consumption of metabolites in response to stimulation, we used significance criteria of $p < 0.05$ and $|FC| > 1$. Of the original 1652 species, 676 metabolites (41.0%) met the significance criteria for HCA-positive samples and 678 (40.9%) for HCA-negative samples.

HCA-positive and -negative samples demonstrated distinct responses to SEB/CD28-induced activation (Fig. 2A). Activation of HCA-negative cultures produced a total of 580 species (three upward arrows in HCA-negative circle in Fig. 2A) and consumed 98 (three downward arrows). One hundred sixty-five of the metabolites produced and 35 consumed were unique to the HCA-negative sample group; that is, these 200 metabolites (29.5%) were not differentially expressed by HCA-positive samples. Likewise, activation of HCA-positive cultures produced a total of 584 metabolites (three upward arrows in HCA-positive circle in Fig. 2A) and consumed 92 (three downward arrows). One hundred sixty-three of the metabolites produced and 35 consumed, for a total of 198 metabolites (29.3%), were unique to the HCA-positive sample group.

As expected, the exometabolomic activity observed in HCA-positive samples showed a large overlap with exometabolomic activity seen in $CD4^+$ T lymphocytes derived from HCA-negative samples: of the 676 species produced or consumed by HCA-positive samples, 478 metabolites (70.7%) were common to both HCA-positive and -negative cultures, with 410 metabolites (60.7%) having the same directionality of change (consumed or produced). Overall, the responses of both sample groups to SEB/CD28 stimulation were dominated by exometabolome increases (i.e., production of metabolites).

Next, we used volcano plot analyses to directly compare the normalized abundance of individual metabolic species between HCA-positive and -negative sample types and highlight individual metabolites that met the significance criteria. Fig. 2B shows two volcano plot analyses that compare all (1652) detected metabolites in the naive (left) and activated states (right). The $\log_2$[FC] is plotted along the *x*-axis (FC = mean $_{HCA\text{-}POS}$/mean $_{HCA\text{-}NEG}$), and the statistical significance of this is shown along the *y*-axis ($-\log_{10}$ scale). Metabolites that display a positive $\log_2$[FC] are overexpressed (i.e., overproduced) in HCA-positive samples, whereas negative values indicate underexpression (i.e., overconsumed) in the HCA-positive sample group. Statistically significant metabolic species ($p < 0.05$) are shown in blue, whereas statistically insignificant species are represented in black. Identified metabolites are displayed in red and labeled.

Altogether, we detected 482 statistically significant species in naive state. Of these, 411 (85.3%) metabolites showed a statistically significant positive $\log_2$[FC]; the remaining 71 (14.7%) species reflected statistically significant negative differences. Comparably, 442 statistically significant species were identified in the activated state. Of these, 376 (85.1%) metabolic species showed a statistically significant positive $\log_2$[FC], whereas 66 (14.9%) exhibited negative differences, suggesting extensive changes in the production and consumption of metabolic species after exposure to HCA.

Identification of metabolic species with immune response modifier potential

In addition, we used volcano plot analyses to produce a list of metabolic species (shown in blue, Fig. 2B) that were prioritized for identification. We putatively identified five metabolites:

Table I. Characteristics of patient samples

Patient ID	Gestational Age (wk, d)	Sex	Race	Delivery Mode	Day of Blood Draw (after Birth)	Exposure to Prenatal Antibiotics	Exposure to Postnatal Antibiotics	Clinical Signs of Funisitis in Fetus
HCA-negative samples (n = 10)								
339	26, 5	M	African American	Cesarean	10	Y	Amp/Gen through DOL 3	N/A
351	25, 5	M	White	Cesarean	5	Y	Amp/Gen through DOL 7	N/A
326	27, 5	M	White	Cesarean	10	Y	Amp/Gen through DOL 2	N/A
245	26, 5	M	White	Cesarean	10	Y	Amp/Gen through DOL 2	N/A
246	26, 5	F	White	Vaginal	10	N	Amp/Gen through DOL 7	N/A
16	26, 5	F	African American	Vaginal	5	Y	Amp/Gen through DOL 2	N/A
235	27, 5	F	White	Cesarean	5	Y	Amp/Gen through DOL 2	N/A
193	27, 5	F	White	Cesarean	10	Y	Amp/Gen through DOL 2	N/A
304	25, 6	F	White	Cesarean	10	Y	Amp/Gen through DOL 6 and Van on DOL 3 only	N/A
252	26, 6	M	White	Cesarean	5	N	Amp/Gen through DOL 3 and Gen DOL 10 only	N/A
HCA-positive samples (n = 10)								
345	27, 5	M	African American	Cesarean	10	Y	Amp/Gen through DOL 6	Stage II FIRS
230	26, 4	M	African American	Vaginal	10	Y	Amp/Gen through DOL 2	None
314	27, 6	M	African American	Vaginal	10	Y	Amp/Gen through DOL 7	Stage II FIRS
305	26, 6	M	White	Cesarean	10	Y	Amp/Gen through DOL 6	None
262	28, 5	F	White	Vaginal	10	Y	Amp/Gen through DOL 9	Stage II FIRS
242	25, 4	F	White	Cesarean	10	Y	Amp/Gen through DOL 7	Stage II FIRS
350	24, 6	F	White	Cesarean	10	Y	Amp through DOL 10 and Gen DOL 6	Stage II FIRS
223	27, 5	F	African American	Vaginal	10	Y	Amp through DOL 10, Gen DOL 3, and Cfp DOL 3–10 only	Stage II FIRS
307	28, 6	M	White	Cesarean	10	Y	Amp/Gen through DOL 6 and Ctx DOL 2	Stage I FIRS
313	25, 5	F	White	Vaginal	10	Y	Amp/Gen through DOL 2 and Gen/Van DOL 9, 10 only	Stage II FIRS
Statistical analyses								
p	0.69	1	0.36	0.18	0.04	0.15	0.03	

Amp, ampicillin; Cfp, cefepime; Ctx, cefotaxime; Gen, gentamicin; N/A, not applicable; Van, vancomycin.

4-hydroxynonenal (4-HNE), 3-hydroxykynurenine (3-HK), dopamine (DA), serotonin (5-HT), and LysoPC [18:2(9Z, 12Z)] (LPC) (Table II).

From the prioritized list of metabolic species, we putatively identified one metabolite 4-HNE (m/z 195.07, RT 1.03 min) that belongs to the glutathione (GSH) detoxification pathway (Supplemental Fig. 3A). GSH levels have previously been shown to be important in determining the course of the adaptive immune response (36). Analysis of 4-HNE in this mass spectrometry revealed relatively lower levels of

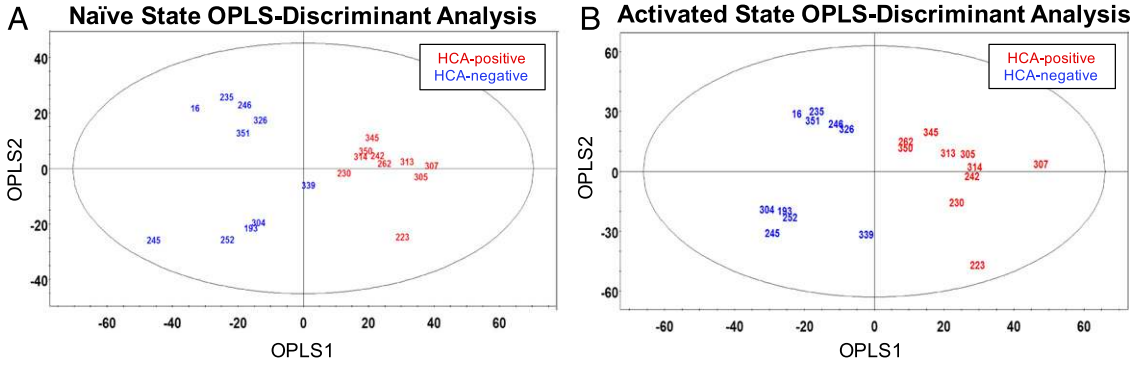

FIGURE 1. Preterm CD4$^+$ T lymphocytes exposed to HCA exhibit distinct exometabolomic profiles in both naive and activated states. (**A**) Left OPLS-DA score plot illustrates the distinct exometabolomic signatures of naive HCA-positive and -negative CD4$^+$ T lymphocytes. Mass spectral data were normalized and Pareto scaled before analysis. OPLS1 resolves the two sample types, explaining 27.8% of the covariance in the data. OPLS2 explains 21.9% of the variance between spectra. The ellipse denotes the 95% significance limit of the model, as defined by Hotelling's t test. This experiment was independently performed once; each UPLC-IM-MS measurement was performed in triplicate (technical replicates). (**B**) Right OPLS-DA score plot illustrates the distinct exometabolomic signatures of activated HCA-positive and -negative CD4$^+$ T lymphocytes. Mass spectral data were normalized and Pareto scaled before analysis. OPLS1 resolves the two sample types, explaining 23.3% of the covariance between spectra. OPLS2 explains 28.6% of the variance between spectra. The ellipse denotes the 95% significance limit of the model, as defined by Hotelling's t test. This experiment was independently performed once; each UPLC-IM-MS measurement was performed in triplicate (technical replicates).

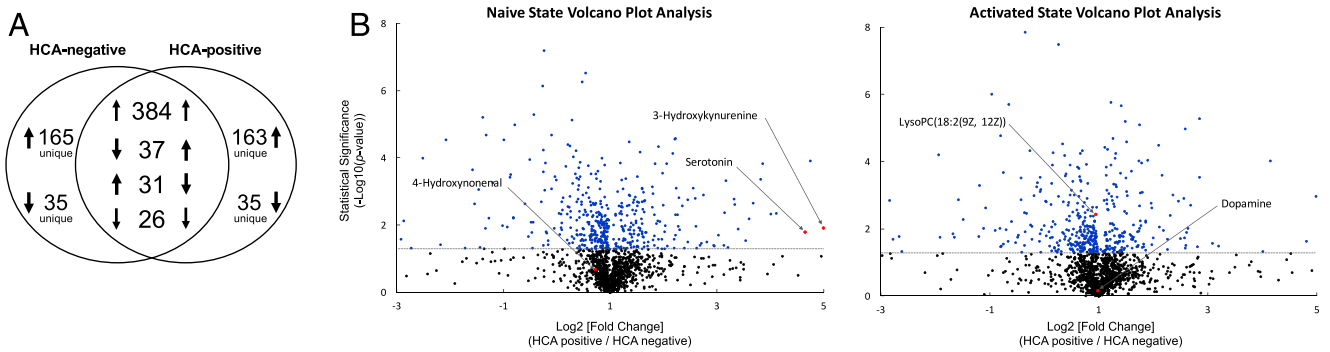

FIGURE 2. Exposure to HCA alters CD4$^+$ T lymphocyte exometabolome production and consumption patterns after SEB/CD28-induced activation. (**A**) Venn diagram illustrating the production and consumption of differentially expressed metabolites ($|FC| > 1$, $p < 0.05$) upon stimulation with SEB/CD28. Numerals denote the number of differentially expressed metabolites, and arrows denote the directionality of change after stimulation. (**B**) Volcano plot analyses of HCA-positive and -negative CD4$^+$ T lymphocyte exometabolome in the naive and activated states. Comparisons of all metabolites from samples exposed to in utero HCA ($n = 10$) and not exposed to HCA ($n = 10$). Volcano plots display the relationship between the $\log_2$[FC] and its statistical significance using a scatterplot view. The *y*-axis represents the negative $\log_{10}$ of *p* values (a higher value indicates greater statistical significance), and the *x*-axis signifies the $\log_2$[FC] (normalized abundance were used to compute these values). Black points indicate metabolites expressed at insignificantly different levels in both sample types ($p > 0.05$). Blue points indicate metabolites expressed at significantly different levels in one sample type over the other ($p < 0.05$). Putatively identified metabolites are shown in red and labeled.

4-HNE in HCA-positive samples in the naive state only (Fig. 3A, 3B). Statistical analyses using the Wilcoxon matched-pairs signed-rank test indicated a statistically significant difference in 4-HNE ($p < 0.05$) in naive state only, suggesting that exposure to HCA may affect the 4-HNE detoxification process before the initiation of an adaptive immune response.

We also observed exometabolome changes in HCA-positive samples relating to the tryptophan metabolism pathway, which has previously been shown to influence the development of the adaptive immune response (37). Both putatively identified metabolites, 5-HT (m/z 177.08, RT 2.57 min) and 3-HK (m/z 225.09, RT 1.25), are downstream metabolites in the tryptophan pathway (Supplemental Fig. 3B).

Overall, 5-HT was elevated in HCA-positive CD4$^+$ T lymphocytes in both naive and activated states (Fig. 4A). Specifically, 9 of the 12 pairs showed greater normalized abundance of 5-HT in the HCA-positive sample in both naive and activated states (Supplemental Fig. 2A). Statistical analyses using the Wilcoxon matched-pairs signed-rank test indicate a significant difference in both naive ($p < 0.01$) and activated ($p < 0.01$) states, suggesting that exposure to HCA may alter 5-HT metabolism before and after the initiation of an adaptive immune response.

The signal for 3-HK was also elevated in HCA-positive CD4$^+$ T lymphocytes in both naive and activated states (Fig. 4B). Specifically, 5 of 12 matched pairs showed increased 3-HK signal in HCA-positive samples in both states (Supplemental Fig. 2B). Statistical analyses using the Wilcoxon matched-pairs signed-rank test indicate a significant difference in both naive ($p < 0.01$) and activated ($p < 0.05$) states, suggesting that exposure to HCA may modify 3-HK metabolism before and after the initiation of an adaptive immune response.

We have also putatively identified DA (m/z 176.07, RT 4.63 min), a metabolite in the catecholamine biosynthesis pathway (Supplemental Fig. 3C), and LPC (m/z 520.35, RT 10.49 min), which is formed through the hydrolysis of phosphatidylcholine by phospholipase A_2 (PLA_2) (Supplemental Fig. 3D). Statistical analyses using the Wilcoxon matched-pairs signed-rank test indicated no overall significant differences in DA (Fig. 5A, Supplemental Fig. 2C) and LPC (Fig. 5B, Supplemental Fig. 2D) levels between HCA-positive and -negative samples in either state, suggesting that exposure to HCA does not impact DA and LPC metabolism in the naive and activated states.

Characterizing the phenotype of CD4$^+$ T lymphocytes and alterations in cytokine production after exposure to HCA

Lastly, we used fluorescence-based flow cytometry to interrogate differences in cell surface marker expression and identify any phenotypic features that may distinguish HCA-positive and HCA-negative CD4$^+$ T lymphocytes. We found the T_H1 phenotype to be overexpressed in HCA-positive samples (Fig. 6A). In addition, we used Luminex assays to determine changes in the cytokine production of activated CD4$^+$ T lymphocytes after exposure to HCA. We found significant increases in IFN-γ production in HCA-positive samples ($p = 0.0032$) (Fig. 6B). Taken together, these data suggest a notable bias toward a T_H1 immune response in HCA-positive preterm infants.

Discussion

Maintenance and regulation of CD4$^+$ T lymphocyte metabolic homeostasis is necessary for producing an effective immune response (38, 39). Historically, fetal cytokine responses have been thought to be biased toward a T_H2 phenotype to protect against fetal rejection (40). In contrast, increased fetal T_H1 cytokine

Table II. List of putatively identified metabolites and their mass accuracy

Feature	Experimental m/z Ratio Pairs	RT (min)	Putative Molecular Identification	Mass Accuracy (ppm)
1	195.07	1.03	4-HNE	12.80
2	177.08	2.57	5-HT	17.00
3	225.09	1.25	3-HK	20.25
4	176.07	4.63	DA	13.10
5	520.35	10.49	LPC	28.04

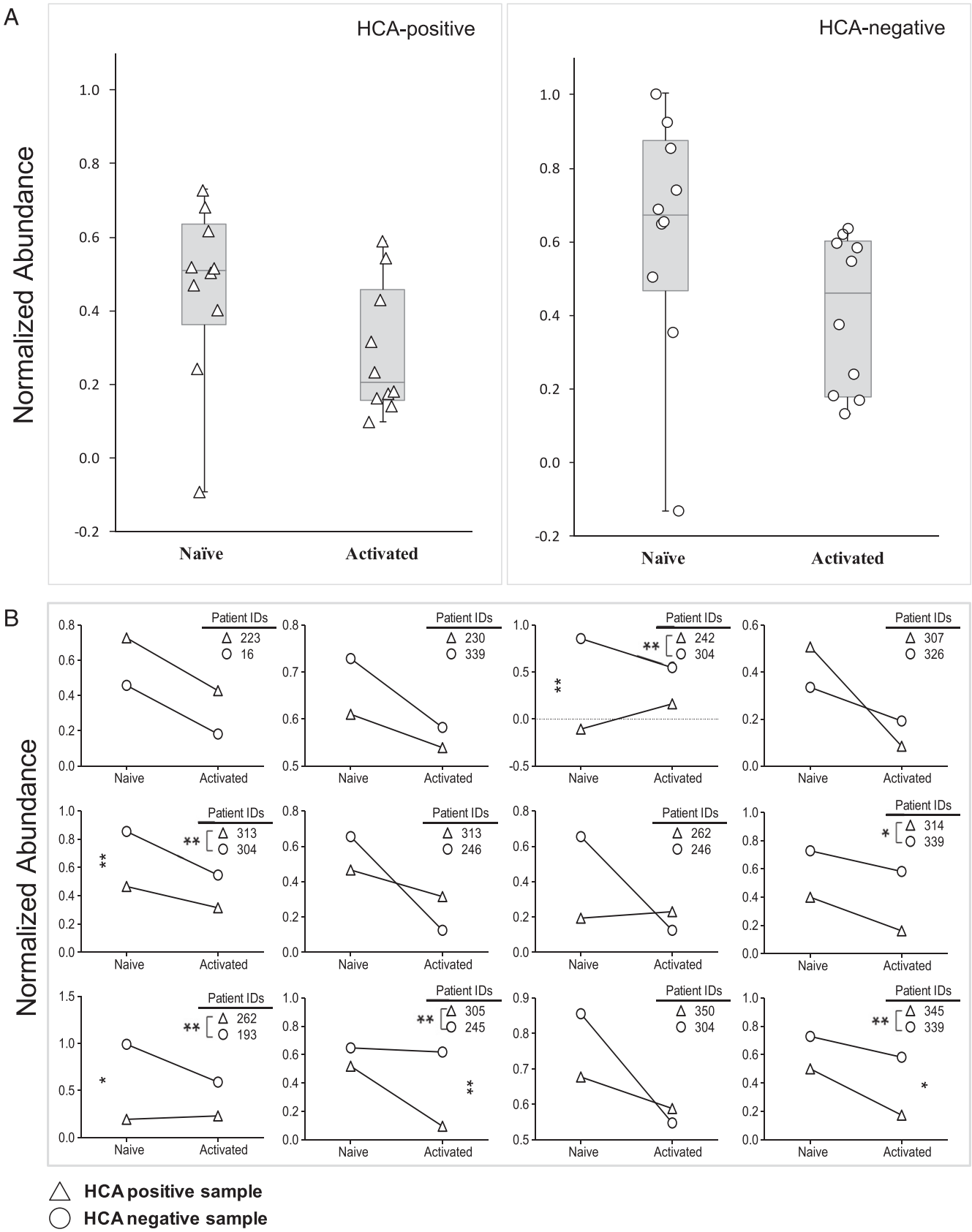

FIGURE 3. Naive CD4$^+$ T lymphocytes exposed to HCA exhibited decreased abundances of 4-HNE. (**A**) Box-and-whisker plot analysis with scatter overlay depicting the normalized abundance values of the putatively identified metabolite, 4-HNE (m/z 195.07, RT 1.03 min). Error bars signify maximum and minimum detected values. HCA-positive samples are denoted by triangles and HCA-negative samples by circles. Median values are also shown. (**B**) Pairwise comparison of the normalized abundance of 4-HNE (m/z 195.07, RT 1.03 min) in the naive and activated states. Each graph depicts the results of two-way repeated-measures ANOVA. HCA-positive samples are represented with triangles, whereas HCA-negative samples are represented by circles. Statistical significance is denoted with asterisks (*$p < 0.05$, **$p < 0.01$).

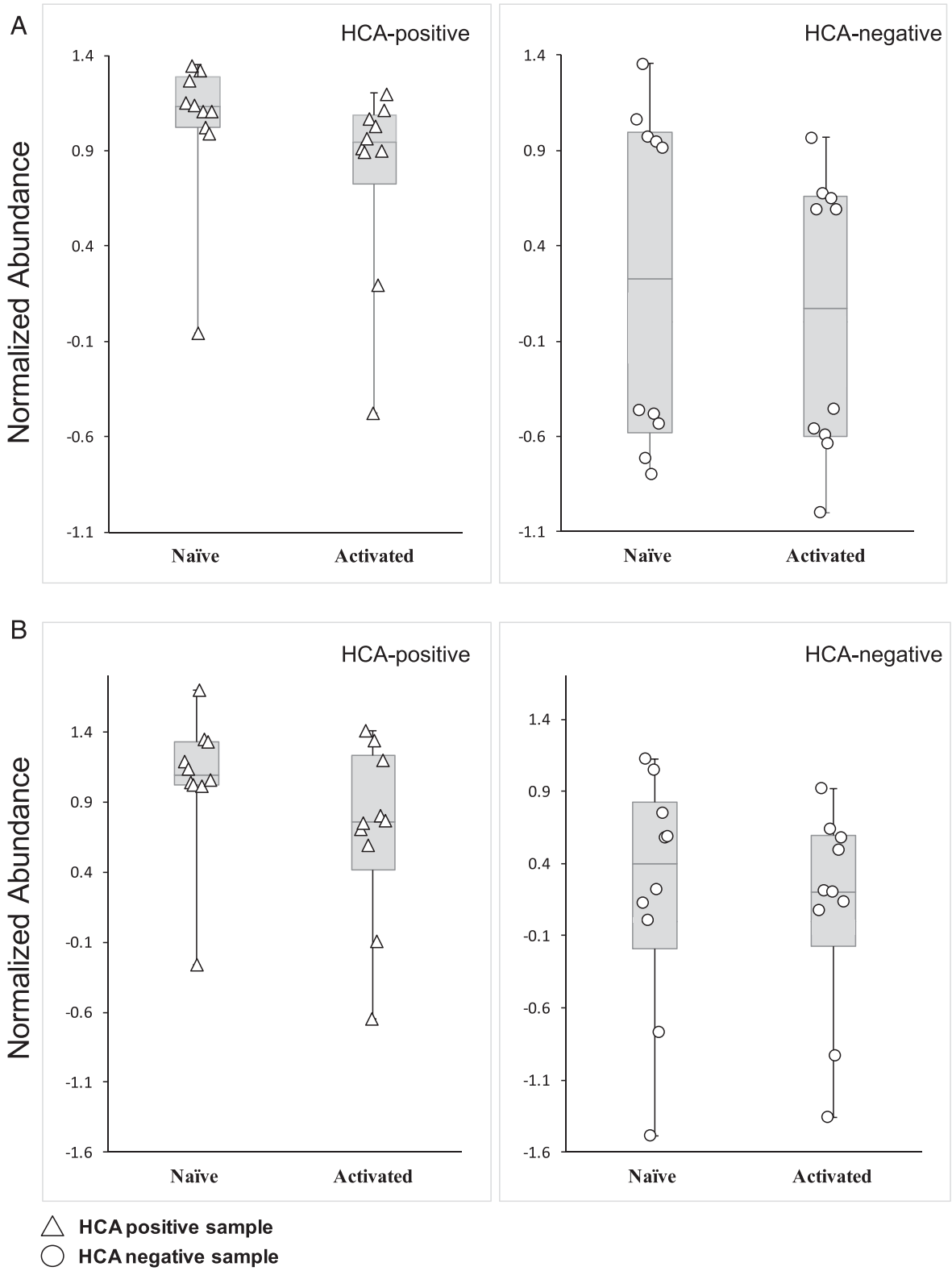

FIGURE 4. Exposure to HCA alters tryptophan metabolism in naive and activated CD4$^+$ T lymphocytes. (**A**) Box-and-whisker plot analysis with scatter overlay depicting the normalized abundance values of the putatively identified metabolite, 5-HT (m/z 177.08, RT 2.57 min). Error bars signify maximum and minimum detected values. HCA-positive samples are denoted by triangles and HCA-negative samples by circles. Median values are also shown. (**B**) Box-and-whisker plot analysis with scatter overlay depicting the normalized abundance values of the putatively identified metabolite, 3-HK (m/z 225.09, RT 1.25 min). Error bars signify maximum and minimum detected values. HCA-positive samples are denoted by triangles and HCA-negative samples by circles. Median values are also shown.

production has been shown to increase the risk for inflammatory injury, but has also been associated with improved immunity toward viral and fungal challenges (41). Thus, a better understanding of mechanisms underlying the CD4$^+$ T lymphocyte exometabolome may help explain the seemingly contradictory outcomes of increased fetal T_H1 cytokine production and also point to

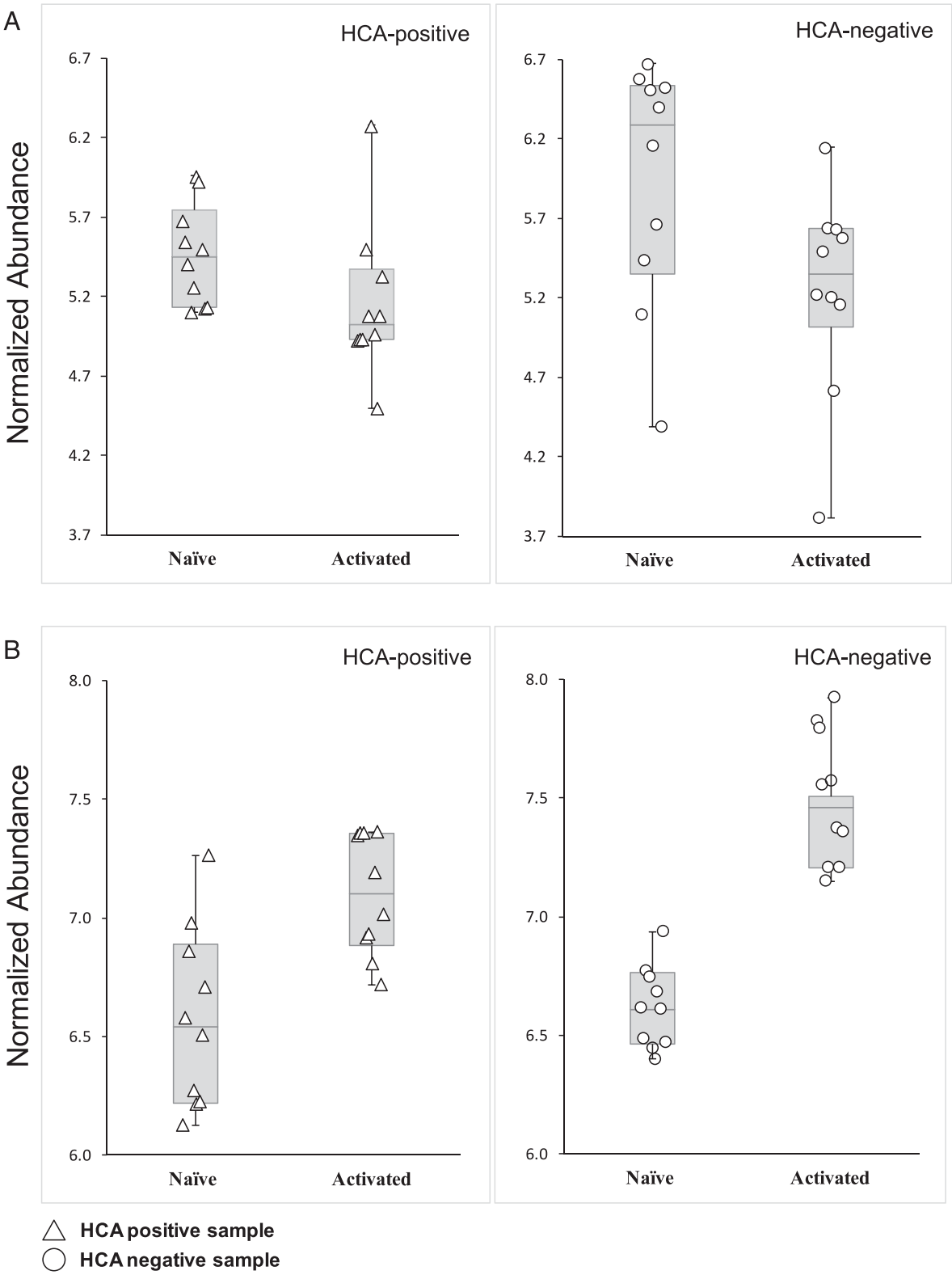

FIGURE 5. Exposure to HCA does not affect DA and LPC metabolism in naive and activated $CD4^+$ T lymphocytes. (**A**) Box-and-whisker plot analyses with scatter overlay depicting the normalized abundance values of the putatively identified metabolite, DA (m/z 176.07, RT 4.63 min). Error bars signify maximum and minimum detected values. HCA-positive samples are denoted by triangles and HCA-negative samples by circles. Median values are also shown. (**B**) Box-and-whisker plot analysis with scatter overlay depicting the normalized abundance values of the putatively identified metabolite, LPC (m/z 520.35, RT 10.49 min). Error bars signify maximum and minimum detected values. HCA-positive samples are denoted by triangles and HCA-negative samples by circles. Median values are also shown.

novel therapeutic targets in the prevention of inflammatory injury after preterm birth and contribute toward the development of treatment options.

We have applied UPLC-IM-MS to produce the first exometabolomic profiles of naive and activated $CD4^+$ T lymphocytes derived from human preterm infants with and without HCA

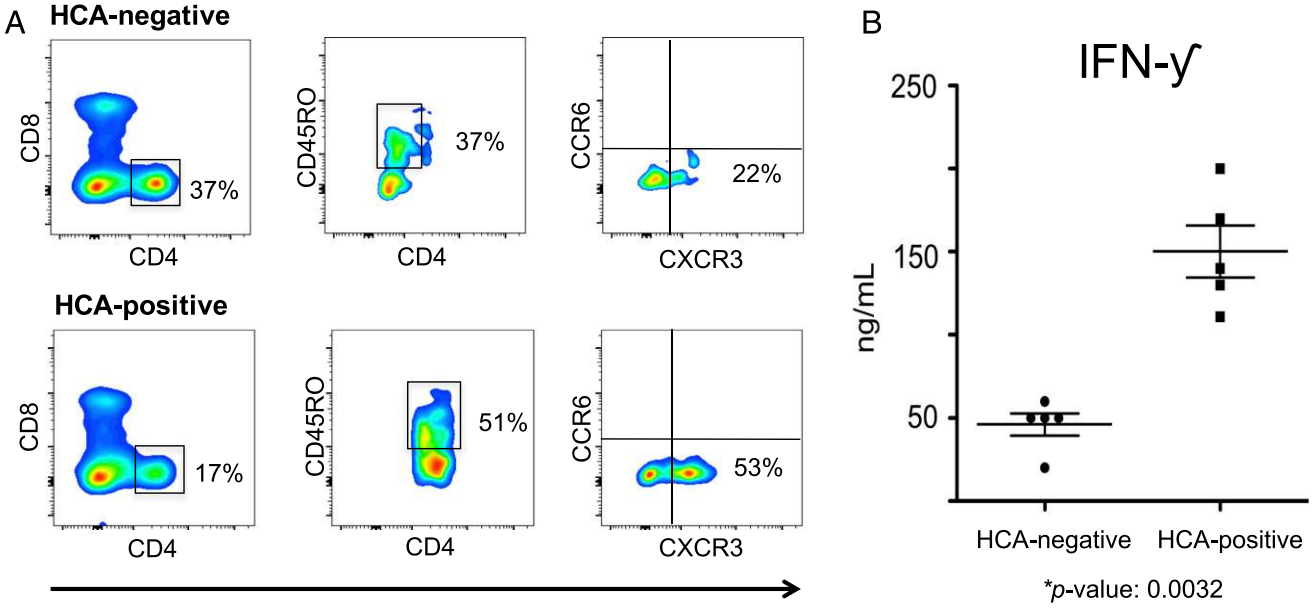

FIGURE 6. Exposure to HCA increases the percentage of memory CD4$^+$ T lymphocytes exhibiting a T_H1 phenotype and IFN-γ secretion. (**A**) Representative analytic flow cytometry plot of CD4$^+$ T lymphocytes collected on postnatal day 10 from five pairs of preterm infants matched for gestational age, day of blood draw, sex, race, prenatal steroid exposure, and delivery mode. Each pair consisted of one HCA-positive and one HCA-negative patient (10 samples total). Data from two 24 wk gestation female Hispanic infants, delivered via cesarean section after prenatal steroid prophylaxis, are shown. One infant was exposed to in utero HCA, whereas the other showed no clinical or histological signs of chorioamnionitis. (**B**) IFN-γ secretions were measured by Luminex technology. Cells were collected from five pairs of preterm infants matched for gestational age, day of blood draw, sex, race, prenatal steroid exposure, and delivery mode. Each pair consisted of one HCA-positive and one HCA-negative patient (10 samples total). Paired *t* test was used to determine statistically significant differences. This experiment was independently performed once, without replicates.

exposure. Although our approach has several limitations, we attempted to carefully match samples for known modulators of immune responses including exposure to prenatal steroids, delivery mode, sex, race, and gestational age. We were not able to rule out other confounding variables, such as maternal smoking (42).

The availability of postnatal blood samples from extremely low-birth-weight infants combined with UPLC-IM-MS methodology did not allow us to test >20 individual patients. However, because we analyzed CD4$^+$ T lymphocyte exometabolomes before and after activation, we were able to collect a large set of data from 40 separate samples. This allowed us to perform the appropriate statistical analyses. Lastly, our in vitro approach may not reflect the complexity of fetal immune activation associated with in vivo HCA exposure (43), but our approach provided a means for determining potentially important metabolites and associated pathways that could be critical to CD4$^+$ T lymphocyte metabolism and function in this vulnerable population, without a priori knowledge.

In utero exposure to HCA is known to prematurely activate the otherwise mostly dormant fetal adaptive immune response (44); however, its postnatal effects on CD4$^+$ T lymphocyte function and metabolism have not yet been discerned. We discovered that exposure to HCA has a substantial and defined overall impact on CD4$^+$ T lymphocyte exometabolomic profiles in both naive and activated states. This could indicate a positive correlation between fetal exposure to HCA and dysregulation of naive CD4$^+$ T lymphocyte bioenergetics that is perpetuated in the activated state. An unexpected finding, however, was the sizable within-group variation exhibited by HCA-negative samples. This variation could be attributed to naturally occurring biological variability; however, it is also possible that exposure to HCA induces a more uniform exometabolomic phenotype. Although the timing of sample collection may explain this intragroup variation, we believe this not to be the case. Studying the postnatal dates of sample collection did not yield any clear patterns of association, and although our sample size is limiting in this regard, we are confident that the date of sample collection did not contribute to this intragroup variation.

Both HCA-positive and -negative samples predominantly increased their metabolite production upon activation, and the numeric extent of metabolite turnover was nearly identical between the two sample types. This large overlap in the levels of exometabolic activity is noteworthy but expected considering that both sample groups are derived from the same cell type. However, despite similarities in the overall exometabolic activity, the production and consumption of specific metabolites in response to SEB/CD28-induced activation varied markedly between HCA-positive and -negative sample types: ∼30% of metabolites produced/consumed were uniquely expressed by CD4$^+$ T lymphocytes derived from HCA-positive infants. This large divergence in the differential expression of specific metabolites supports a correlation between in utero HCA exposure and changes in the bioenergetics of naive and activated CD4$^+$ T lymphocytes.

In follow-up analyses of the exometabolomic overlap, we were able to discern additional distinctions in the differential expression levels of metabolites common to both sample types. Almost 60% of the metabolites differentially expressed by both sample groups were either overexpressed or underexpressed by the HCA-positive sample group. These data indicate a connection between HCA exposure and metabolic dysregulation of fetal CD4$^+$ T lymphocytes.

We have putatively identified five distinct metabolites that, with further validation, could function as biomarkers of HCA exposure. These include 4-HNE, 5-HT, 3-HK, DA, and LPC. 4-HNE is widely known as an inducer of oxidative stress and a highly toxic end product of lipid peroxidation (45–47). Thus, precise regulation of intracellular 4-HNE levels is necessary for cell survival. This molecule is largely depleted through GSH conjugation, which is catalyzed by GST (48, 49). Consequently, the neutralization/

detoxification process has been shown to be highly dependent on GSH levels (50). Current evidence suggests that GSH is also of great importance to the initiation and progression of $CD4^+$ T lymphocyte activation (51–54). Recent studies even point to a correlation between GSH deficiency and decreased levels of T_H1-associated cytokines (IL-2 and IFN-γ) (55).

Our findings indicate decreased abundances of 4-HNE in HCA-positive $CD4^+$ T lymphocytes in the naive state only. This discrepancy in 4-HNE levels may be because of increased GSH levels (and therefore increased rates of detoxification) in naive HCA-positive samples. Although we are not certain as to why GSH levels would be selectively increased in the naive state, this finding is consistent with existing data that suggest changes in GSH concentration can affect activation-dependent lymphocyte proliferation without regulating the activated functions of these cells (56).

In addition to altered 4-HNE metabolism, we observed changes in two metabolites that belong to the tryptophan metabolism pathway. As downstream metabolites of tryptophan, 5-HT and 3-HK abundances are directly indicative of tryptophan degradation patterns (57). Existing data suggest a strong correlation between IFN-γ production and sustained upregulation of tryptophan degradation (58–61). Posited as the *tryptophan depletion theory*, the details of this connection are not thoroughly understood, although it is thought that IFN-γ production precipitates this upregulation (62). IFN-γ is a hallmark proinflammatory cytokine classically associated with the T_H1 adaptive immune response (63, 64). In follow-up experiments, we have identified statistically significant increases in IFN-γ production in activated $CD4^+$ T lymphocytes exposed to HCA, supporting our findings on changes to tryptophan degradation in HCA-positive $CD4^+$ T lymphocytes.

Our observations of increased 5-HT and 3-HK abundances in conjunction with amplified IFN-γ production in HCA-positive samples suggest that exposure to HCA may be associated with the upregulation of tryptophan degradation in naive and activated $CD4^+$ T lymphocytes. Consequently, our data may indicate a correlation between HCA exposure and a T_H1 polarization of the fetal adaptive immune response.

We have also identified DA, a metabolite that belongs to the norepinephrine and epinephrine biosynthesis pathway. These two catecholamines have been shown to regulate lymphocyte function in vitro (65, 66). As the immediate precursor to norepinephrine (NE) and the preferential method for its synthesis, DA abundances are directly indicative of NE biosynthesis patterns (67). Mouse studies have previously shown the production of catecholamines, including NE and epinephrine, to have an important role in modulating T lymphocyte–mediated immune responses (68, 69). In fact, elevated levels of these catecholamines in resting T lymphocytes have been shown to decrease production of IL-12 (a T_H1-promoting cytokine) (70). Greater abundances of catecholamines in activated T lymphocytes are also known to impair the function of human effector T_H1 lymphocytes by suppressing IFN-γ and IL-2 (proinflammatory cytokines) production and enhance the production of T_H2 (anti-inflammatory) cytokines (67, 71, 72). Therefore, it was not surprising for us to find comparable abundances of DA in naive and activated HCA-positive and -negative samples. Our observations suggest that exposure to HCA does not impact DA metabolism in naive or activated $CD4^+$ T lymphocytes. This may be because HCA exposure induces a T_H1 polarization of the fetal adaptive immune response, and normal catecholamine production is requisite for this type of immune response.

Lastly, we have also identified LPC, a bioactive proinflammatory lipid produced via the hydrolysis of plasma membrane phosphatidylcholine, a process catalyzed by the PLA_2 enzyme (73). Obstruction of this enzymatic function in animal models has been shown to diminish the development of T_H1 and T_H17 immune responses (74). Mouse studies from the same research group have also shown cytosolic PLA_2-deficient mice to be incapable of producing T_H1 type cytokines (75). Considering our findings of comparable LPC abundances in naive and activated HCA-positive and -negative samples, we believe HCA exposure does not impact LPC metabolism. This may be because in utero HCA exposure induces a T_H1 polarization of the fetal adaptive immune response, and consistent LPC metabolism is necessary for the initiation and production of this immune response.

A suitable balance between T_H1 and T_H2 adaptive immune responses that meets the immune challenge is necessary to avoid excessive inflammation/tissue damage (T_H1) and the over-promotion of allergic responses (T_H2) (76). Preterm infants with evidence of perinatal infection exhibit a higher proportion of T_H1 cells than uninfected preterm infants (77), suggesting that exposure to HCA polarizes the fetal adaptive immune response toward the T_H1 type. Within the noted limitations of our study, our findings may indicate a possible mechanistic link between in utero HCA exposure and T_H1 polarization of the fetal adaptive immune response. Validation studies will be necessary to confirm the immune biomarker role of the putatively identified metabolites in our study.

To summarize our results, we have shown for the first time, to our knowledge, that antenatal exposure to HCA induces changes in the bioenergetics of naive and activated $CD4^+$ T lymphocytes of preterm infants, resulting in an altered exometabolomic profile. Putatively identified metabolites differentially secreted by HCA-positive $CD4^+$ T lymphocytes support existing literature, suggesting that exposure to HCA polarizes the adaptive immune response toward a T_H1 response. In addition to inflammatory injury associated with preterm birth, metabolic changes to the fetal immune processes resulting from in utero HCA exposure may explain the observed immune dysregulation we observed in this study, suggesting a critical role for the fetal environment in shaping normal and aberrant host responses of the developing infant.

Acknowledgments

We appreciate the support of the SyBBURE-Searle Undergraduate Research Program, the Vanderbilt Institute for Integrative Biosystems Research and Education, and the Vanderbilt Center for Innovative Technology. Additionally, we acknowledge and thank Dr. John P. Wikswo of Vanderbilt Institute for Integrative Biosystems Research and Education for support and valuable comments.

Disclosures

The authors have no financial conflicts of interest.

References

1. Martin, J. A.; National Center for Health Statistics. 2005. *Births: Final Data for 2003*. US Department of Health and Human Services, Centers for Disease Control and Prevention, National Center for Health Statistics, Washington, DC.
2. Beck, S., D. Wojdyla, L. Say, A. P. Betran, M. Merialdi, J. H. Requejo, C. Rubens, R. Menon, and P. F. Van Look. 2010. The worldwide incidence of preterm birth: a systematic review of maternal mortality and morbidity. *Bull. World Health Organ.* 88: 31–38.
3. Tucker, J. M., R. L. Goldenberg, R. O. Davis, R. L. Copper, C. L. Winkler, and J. C. Hauth. 1991. Etiologies of preterm birth in an indigent population: is prevention a logical expectation? *Obstet. Gynecol.* 77: 343–347.
4. Hillier, S. L., J. Martius, M. Krohn, N. Kiviat, K. K. Holmes, and D. A. Eschenbach. 1988. A case-control study of chorioamnionic infection and histologic chorioamnionitis in prematurity. *N. Engl. J. Med.* 319: 972–978.
5. Goldenberg, R. L., J. C. Hauth, and W. W. Andrews. 2000. Intrauterine infection and preterm delivery. *N. Engl. J. Med.* 342: 1500–1507.
6. Steel, J. H., S. Malatos, N. Kennea, A. D. Edwards, L. Miles, P. Duggan, P. R. Reynolds, R. G. Feldman, and M. H. Sullivan. 2005. Bacteria and

inflammatory cells in fetal membranes do not always cause preterm labor. *Pediatr. Res.* 57: 404–411.
7. Yoon, B. H., R. Romero, J. B. Moon, S.-S. Shim, M. Kim, G. Kim, and J. K. Jun. 2001. Clinical significance of intra-amniotic inflammation in patients with preterm labor and intact membranes. *Am. J. Obstet. Gynecol.* 185: 1130–1136.
8. Gotsch, F., R. Romero, J. P. Kusanovic, S. Mazaki-Tovi, B. L. Pineles, O. Erez, J. Espinoza, and S. S. Hassan. 2007. The fetal inflammatory response syndrome. *Clin. Obstet. Gynecol.* 50: 652–683.
9. Andrews, W. W., R. L. Goldenberg, O. Faye-Petersen, S. Cliver, A. R. Goepfert, and J. C. Hauth. 2006. The Alabama Preterm Birth study: polymorphonuclear and mononuclear cell placental infiltrations, other markers of inflammation, and outcomes in 23- to 32-week preterm newborn infants. *Am. J. Obstet. Gynecol.* 195: 803–808.
10. Weitkamp, J. H., S. O. Guthrie, H. R. Wong, L. L. Moldawer, H. V. Baker, and J. L. Wynn. 2016. Histological chorioamnionitis shapes the neonatal transcriptomic immune response. *Early Hum. Dev.* 98: 1–6.
11. Gomez, R., R. Romero, F. Ghezzi, B. H. Yoon, M. Mazor, and S. M. Berry. 1998. The fetal inflammatory response syndrome. *Am. J. Obstet. Gynecol.* 179: 194–202.
12. Chen, M. L., E. N. Allred, J. L. Hecht, A. Onderdonk, D. VanderVeen, D. K. Wallace, A. Leviton, and O. Dammann, ELGAN Study. 2011. Placenta microbiology and histology and the risk for severe retinopathy of prematurity. *Invest. Ophthalmol. Vis. Sci.* 52: 7052–7058.
13. Wu, Y. W., and J. M. Colford, Jr. 2000. Chorioamnionitis as a risk factor for cerebral palsy: a meta-analysis. *JAMA* 284: 1417–1424.
14. Romero, R., J. Espinoza, L. F. Gonçalves, R. Gomez, L. Medina, M. Silva, T. Chaiworapongsa, B. H. Yoon, F. Ghezzi, W. Lee, et al. 2004. Fetal cardiac dysfunction in preterm premature rupture of membranes. *J. Matern. Fetal Neonatal Med.* 16: 146–157.
15. Kramer, B. W., S. Kallapur, J. Newnham, and A. H. Jobe. 2009. Prenatal inflammation and lung development. *Semin. Fetal Neonatal Med.* 14: 2–7.
16. Leviton, A., J. L. Hecht, E. N. Allred, H. Yamamoto, R. N. Fichorova, and O. Dammann, ELGAN Study Investigators. 2011. Persistence after birth of systemic inflammation associated with umbilical cord inflammation. *J. Reprod. Immunol.* 90: 235–243.
17. O'Shea, T. M., E. N. Allred, K. C. Kuban, O. Dammann, N. Paneth, R. Fichorova, D. Hirtz, and A. Leviton, Extremely Low Gestational Age Newborn (ELGAN) Study Investigators. 2012. Elevated concentrations of inflammation-related proteins in postnatal blood predict severe developmental delay at 2 years of age in extremely preterm infants. *J. Pediatr.* 160: 395–401.e4.
18. Bastek, J. A., A. L. Weber, M. A. McShea, M. E. Ryan, and M. A. Elovitz. 2014. Prenatal inflammation is associated with adverse neonatal outcomes. *Am. J. Obstet. Gynecol.* 210: 450.e1–450.e10.
19. Savasan, Z. A., T. Chaiworapongsa, R. Romero, Y. Hussein, J. P. Kusanovic, Y. Xu, Z. Dong, C. J. Kim, and S. S. Hassan. 2012. Interleukin-19 in fetal systemic inflammation. *J. Matern. Fetal Neonatal Med.* 25: 995–1005.
20. Kallapur, S. G., P. Presicce, C. M. Rueda, A. H. Jobe, and C. A. Chougnet. 2014. Fetal immune response to chorioamnionitis. *Semin. Reprod. Med.* 32: 56–67.
21. Vlassaks, E., A. W. Gavilanes, V. Bieghs, A. Reinartz, N. Gassler, P. J. Van Gorp, M. J. Gijbels, O. Bekers, L. J. Zimmermann, J. J. Pillow, et al. 2012. Antenatal exposure to chorioamnionitis affects lipid metabolism in 7-week-old sheep. *J. Dev. Orig. Health Dis.* 3: 103–110.
22. Matsuoka, T., T. Matsubara, K. Katayama, K. Takeda, M. Koga, and S. Furukawa. 2001. Increase of cord blood cytokine-producing T cells in intrauterine infection. *Pediatr. Int.* 43: 453–457.
23. Michalek, R. D., V. A. Gerriets, S. R. Jacobs, A. N. Macintyre, N. J. MacIver, E. F. Mason, S. A. Sullivan, A. G. Nichols, and J. C. Rathmell. 2011. Cutting edge: distinct glycolytic and lipid oxidative metabolic programs are essential for effector and regulatory CD4+ T cell subsets. *J. Immunol.* 186: 3299–3303.
24. Fernandez-Sesma, A., S. Marukian, B. J. Ebersole, D. Kaminski, M. S. Park, T. Yuen, S. C. Sealfon, A. García-Sastre, and T. M. Moran. 2006. Influenza virus evades innate and adaptive immunity via the NS1 protein. *J. Virol.* 80: 6295–6304.
25. Espinosa, E., C. E. Ormsby, G. Reyes-Terán, R. Asaad, S. F. Sieg, and M. M. Lederman. 2010. Dissociation of CD154 and cytokine expression patterns in $CD38^+$ $CD4^+$ memory T cells in chronic HIV-1 infection. *J. Acquir. Immune Defic. Syndr.* 55: 439–445.
26. Kruisbeek, A. M., E. Shevach, and A. M. Thornton. 2004. Proliferative assays for T cell function. *Curr. Protoc. Immunol.* Chapter 3: Unit 3.12.
27. Brown, J. A., S. D. Sherrod, C. R. Goodwin, B. Brewer, L. Yang, K. A. Garbett, D. Li, J. A. McLean, J. P. Wikswo, and K. Mirnics. 2014. Metabolic consequences of interleukin-6 challenge in developing neurons and astroglia. *J. Neuroinflammation* 11: 183.
28. Kessner, D., M. Chambers, R. Burke, D. Agus, and P. Mallick. 2008. ProteoWizard: open source software for rapid proteomics tools development. *Bioinformatics* 24: 2534–2536.
29. Wishart, D. S. 2007. Current progress in computational metabolomics. *Brief. Bioinform.* 8: 279–293.
30. Smith, C. A., G. O'Maille, E. J. Want, C. Qin, S. A. Trauger, T. R. Brandon, D. E. Custodio, R. Abagyan, and G. Siuzdak. 2005. METLIN: a metabolite mass spectral database. *Ther. Drug Monit.* 27: 747–751.
31. Sud, M., E. Fahy, D. Cotter, A. Brown, E. A. Dennis, C. K. Glass, A. H. Merrill, Jr., R. C. Murphy, C. R. Raetz, D. W. Russell, and S. Subramaniam. 2007. LMSD: LIPID MAPS structure database. *Nucleic Acids Res.* 35: D527–D532.
32. Avula, B., Y. H. Wang, G. Isaac, J. Yuk, M. Wrona, K. Yu, and I. A. Khan. 2016. Metabolomics based UHPLC-QToF-MS approach for the authentication of various botanicals and dietary supplements. *Planta Med.* 82: OA13.
33. Korn, T., J. Reddy, W. Gao, E. Bettelli, A. Awasthi, T. R. Petersen, B. T. Bäckström, R. A. Sobel, K. W. Wucherpfennig, T. B. Strom, et al. 2007. Myelin-specific regulatory T cells accumulate in the CNS but fail to control autoimmune inflammation. *Nat. Med.* 13: 423–431.
34. Zhang, X., B. Mozeleski, S. Lemoine, E. Dériaud, A. Lim, D. Zhivaki, E. Azria, C. Le Ray, G. Roguet, O. Launay, et al. 2014. CD4 T cells with effector memory phenotype and function develop in the sterile environment of the fetus. *Sci. Transl. Med.* 6: 238ra72.
35. Weitkamp, J. H., T. Koyama, M. T. Rock, H. Correa, J. A. Goettel, P. Matta, K. Oswald-Richter, M. J. Rosen, B. G. Engelhardt, D. J. Moore, and D. B. Polk. 2013. Necrotising enterocolitis is characterised by disrupted immune regulation and diminished mucosal regulatory (FOXP3)/effector (CD4, CD8) T cell ratios. *Gut* 62: 73–82.
36. Guerra, C., D. Morris, A. Sipin, S. Kung, M. Franklin, D. Gray, M. Tanzil, F. Guilford, F. T. Khasawneh, and V. Venketaraman. 2011. Glutathione and adaptive immune responses against *Mycobacterium tuberculosis* infection in healthy and HIV infected individuals. *PLoS One* 6: e28378.
37. Munn, D. H., and A. L. Mellor. 2013. Indoleamine 2,3 dioxygenase and metabolic control of immune responses. *Trends Immunol.* 34: 137–143.
38. Buck, M. D., D. O'Sullivan, and E. L. Pearce. 2015. T cell metabolism drives immunity. *J. Exp. Med.* 212: 1345–1360.
39. Michalek, R. D., and J. C. Rathmell. 2010. The metabolic life and times of a T-cell. *Immunol. Rev.* 236: 190–202.
40. Härtel, C., N. Adam, T. Strunk, P. Temming, M. Müller-Steinhardt, and C. Schultz. 2005. Cytokine responses correlate differentially with age in infancy and early childhood. *Clin. Exp. Immunol.* 142: 446–453.
41. Maródi, L. 2006. Innate cellular immune responses in newborns. *Clin. Immunol.* 118: 137–144.
42. Herberth, G., M. Bauer, M. Gasch, D. Hinz, S. Röder, S. Olek, T. Kohajda, U. Rolle-Kampczyk, M. von Bergen, U. Sack, et al; Lifestyle and Environmental Factors and Their Influence on Newborns Allergy Risk study group. 2014. Maternal and cord blood miR-223 expression associates with prenatal tobacco smoke exposure and low regulatory T-cell numbers. *J. Allergy Clin. Immunol.* 133: 543–550.
43. Kallapur, S. G., P. Presicce, P. Senthamaraikannan, M. Alvarez, A. F. Tarantal, L. M. Miller, A. H. Jobe, and C. A. Chougnet. 2013. Intra-amniotic IL-1β induces fetal inflammation in rhesus monkeys and alters the regulatory T cell/IL-17 balance. *J. Immunol.* 191: 1102–1109.
44. Luciano, A. A., H. Yu, L. W. Jackson, L. A. Wolfe, and H. B. Bernstein. 2011. Preterm labor and chorioamnionitis are associated with neonatal T cell activation. *PLoS One* 6: e16698.
45. Uchida, K. 2003. 4-Hydroxy-2-nonenal: a product and mediator of oxidative stress. *Prog. Lipid Res.* 42: 318–343.
46. Esterbauer, H., R. J. Schaur, and H. Zollner. 1991. Chemistry and biochemistry of 4-hydroxynonenal, malonaldehyde and related aldehydes. *Free Radic. Biol. Med.* 11: 81–128.
47. Esterbauer, H., P. Eckl, and A. Ortner. 1990. Possible mutagens derived from lipids and lipid precursors. *Mutat. Res.* 238: 223–233.
48. Awasthi, Y. C., Y. Yang, N. K. Tiwari, B. Patrick, A. Sharma, J. Li, and S. Awasthi. 2004. Regulation of 4-hydroxynonenal-mediated signaling by glutathione S-transferases. *Free Radic. Biol. Med.* 37: 607–619.
49. Spitz, D. R., S. J. Sullivan, R. R. Malcolm, and R. J. Roberts. 1991. Glutathione dependent metabolism and detoxification of 4-hydroxy-2-nonenal. *Free Radic. Biol. Med.* 11: 415–423.
50. Yadav, U. C., K. V. Ramana, Y. C. Awasthi, and S. K. Srivastava. 2008. Glutathione level regulates HNE-induced genotoxicity in human erythroleukemia cells. *Toxicol. Appl. Pharmacol.* 227: 257–264.
51. Hamilos, D. L., and H. J. Wedner. 1985. The role of glutathione in lymphocyte activation. I. Comparison of inhibitory effects of buthionine sulfoximine and 2-cyclohexene-1-one by nuclear size transformation. *J. Immunol.* 135: 2740–2747.
52. Fischman, C. M., M. C. Udey, M. Kurtz, and H. J. Wedner. 1981. Inhibition of lectin-induced lymphocyte activation by 2-cyclohexene-1-one: decreased intracellular glutathione inhibits an early event in the activation sequence. *J. Immunol.* 127: 2257–2262.
53. Wedner, H. J., G. Bahn, L. K. Gordon, and C. M. Fischman. 1985. Inhibition of lectin-induced lymphocyte activation by 2-cyclohexene-1-one: analysis of DNA synthesis in individual cells by BUdR quenching of Hoechst 33258. *Int. J. Immunopharmacol.* 7: 25–30.
54. Dröge, W., C. Pottmeyer-Gerber, H. Schmidt, and S. Nick. 1986. Glutathione augments the activation of cytotoxic T lymphocytes in vivo. *Immunobiology* 172: 151–156.
55. Peterson, J. D., L. A. Herzenberg, K. Vasquez, and C. Waltenbaugh. 1998. Glutathione levels in antigen-presenting cells modulate Th1 versus Th2 response patterns. *Proc. Natl. Acad. Sci. USA* 95: 3071–3076.
56. Smyth, M. J. 1991. Glutathione modulates activation-dependent proliferation of human peripheral blood lymphocyte populations without regulating their activated function. *J. Immunol.* 146: 1921–1927.
57. Keszthelyi, D., F. J. Troost, and A. A. Masclee. 2009. Understanding the role of tryptophan and serotonin metabolism in gastrointestinal function. *Neurogastroenterol. Motil.* 21: 1239–1249.
58. Werner, E. R., G. Werner-Felmayer, D. Fuchs, A. Hausen, G. Reibnegger, and H. Wachter. 1989. Parallel induction of tetrahydrobiopterin biosynthesis and indoleamine 2,3-dioxygenase activity in human cells and cell lines by interferon-gamma. *Biochem. J.* 262: 861–866.
59. Yoshida, R., T. Nukiwa, Y. Watanabe, M. Fujiwara, F. Hirata, and O. Hayaishi. 1980. Regulation of indoleamine 2,3-dioxygenase activity in the small intestine and the epididymis of mice. *Arch. Biochem. Biophys.* 203: 343–351.

60. Yoshida, R., J. Imanishi, T. Oku, T. Kishida, and O. Hayaishi. 1981. Induction of pulmonary indoleamine 2,3-dioxygenase by interferon. *Proc. Natl. Acad. Sci. USA* 78: 129–132.
61. Grant, R. S., H. Naif, M. Espinosa, and V. Kapoor. 2000. IDO induction in IFN-gamma activated astroglia: a role in improving cell viability during oxidative stress. *Redox Rep.* 5: 101–104.
62. Moffett, J. R., and M. A. A. Namboodiri. 2003. Tryptophan and the immune response. *Immunol. Cell Biol.* 81: 247–265.
63. Mosmann, T. R., and R. L. Coffman. 1989. Heterogeneity of cytokine secretion patterns and functions of helper T cells. *Adv. Immunol.* 46: 111–147.
64. Mosmann, T. R., and S. Sad. 1996. The expanding universe of T-cell subsets: Th1, Th2 and more. *Immunol. Today* 17: 138–146.
65. Cook-Mills, J. M., R. L. Cohen, R. L. Perlman, and D. A. Chambers. 1995. Inhibition of lymphocyte activation by catecholamines: evidence for a non-classical mechanism of catecholamine action. *Immunology* 85: 544–549.
66. Bergquist, J., A. Tarkowski, R. Ekman, and A. Ewing. 1994. Discovery of endogenous catecholamines in lymphocytes and evidence for catecholamine regulation of lymphocyte function via an autocrine loop. *Proc. Natl. Acad. Sci. USA* 91: 12912–12916.
67. Swanson, M. A., W. T. Lee, and V. M. Sanders. 2001. IFN-γ production by Th1 cells generated from naive CD4+ T cells exposed to norepinephrine. *J. Immunol.* 166: 232–240.
68. Josefsson, E., J. Bergquist, R. Ekman, and A. Tarkowski. 1996. Catecholamines are synthesized by mouse lymphocytes and regulate function of these cells by induction of apoptosis. *Immunology* 88: 140–146.
69. Alaniz, R. C., S. A. Thomas, M. Perez-Melgosa, K. Mueller, A. G. Farr, R. D. Palmiter, and C. B. Wilson. 1999. Dopamine beta-hydroxylase deficiency impairs cellular immunity. *Proc. Natl. Acad. Sci. USA* 96: 2274–2278.
70. Klesney-Tait, J., I. R. Turnbull, and M. Colonna. 2006. The TREM receptor family and signal integration. *Nat. Immunol.* 7: 1266–1273.
71. Wahle, M., G. Hanefeld, S. Brunn, R. H. Straub, U. Wagner, A. Krause, H. Häntzschel, and C. G. Baerwald. 2006. Failure of catecholamines to shift T-cell cytokine responses toward a Th2 profile in patients with rheumatoid arthritis. *Arthritis Res. Ther.* 8: R138.
72. Herwald, H., and A. Egesten. 2011. *Sepsis – Pro-inflammatory and Anti-inflammatory Responses.* Karger Medical and Scientific Publishers, Basel, Switzerland.
73. Mehta, D. 2005. Lysophosphatidylcholine: an enigmatic lysolipid. *Am. J. Physiol. Lung Cell. Mol. Physiol.* 289: L174–L175.
74. Marusic, S., P. Thakker, J. W. Pelker, N. L. Stedman, K. L. Lee, J. C. McKew, L. Han, X. Xu, S. F. Wolf, A. J. Borey, et al. 2008. Blockade of cytosolic phospholipase A2 alpha prevents experimental autoimmune encephalomyelitis and diminishes development of Th1 and Th17 responses. *J. Neuroimmunol.* 204: 29–37.
75. Marusic, S., M. W. Leach, J. W. Pelker, M. L. Azoitei, N. Uozumi, J. Cui, M. W. Shen, C. M. DeClercq, J. S. Miyashiro, B. A. Carito, et al. 2005. Cytosolic phospholipase A2 alpha-deficient mice are resistant to experimental autoimmune encephalomyelitis. *J. Exp. Med.* 202: 841–851.
76. Berger, A. 2000. Th1 and Th2 responses: what are they? *BMJ* 321: 424.
77. Melville, J. M., and T. J. Moss. 2013. The immune consequences of preterm birth. *Front. Neurosci.* 7: 79.